Applied Mathematical Biosystems, Volume 1, Issue 1, (Jul-Dec 2025), 38-49

Applied Mathematical Biosystems

journal homepage: https://ambjournal.com

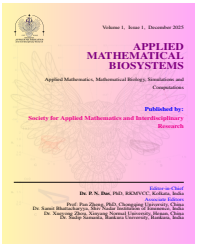

Optimal Strategies for Controlling Visceral Leishmaniasis: A Case Study from South Sudan

Santanu Biswas[1,†], Humaira Aslam[2,†], Suvendu Roy[3], Krishna Pada Das[4] and Md Saifuddin[5]

[1]*Ramakrishna Mission Vivekananda Centenary College, Rahara, Kolkata, West Bengal, India*
[2]*Department Of Mathematics, Adamas University, Barasat - Barrackpore Road, Jagannathpur, Kolkata, West Bengal,India*
[3]*Ramakrishna Mission Vivekananda Centenary College, Rahara, Kolkata, West Bengal, India*
[4]*Mahadevananda Mahavidyalaya, Barrackpore, Kolkata, West Bengal, India*
[5]*Bidhan Chandra College Rishra, Kolkata, West Bengal, India*
[†]*The authors have contributed equally to this work*

Abstract

This study aims to develop and analyze a compartmental model for Visceral Leishmaniasis (VL). The model is calibrated using monthly incidence data from South Sudan for the year 2011. We derive and estimate the basic reproduction number, $\mathcal{R}_0$, for the proposed model and explore the possibility of bifurcation within the system. Various control strategies are examined using optimal control theory, including the use of treated bed nets, vaccination, reservoir culling, and treatment of infected individuals. Numerical simulations indicate that a combined approach involving mass treatment, vaccination, bed nets, and reservoir culling is most effective in reducing VL prevalence. Among these, mass treatment emerges as the most critical intervention during outbreaks. Conversely, relying solely on reservoir culling is unlikely to significantly benefit the community.

Keywords: *Visceral Leishmaniasis; Basic Reproduction Number; Backward Bifurcation; Intervention Strategies.*

Corresponding author: Humaira Aslam *E-mail address:* humairaaslam1694@gmail.com
Received: November 10, 2025 **Revised:** December 23, 2025 **Accepted:** December 27, 2025 **Published:** December 29, 2025

1. INTRODUCTION

Leishmaniasis is recognized as the second most prevalent vector-borne parasitic disease globally. Among its various forms, Visceral Leishmaniasis (VL), Post-Kala-Azar Dermal Leishmaniasis (PKDL), Cutaneous Leishmaniasis (CL), and Mucocutaneous Leishmaniasis are the most commonly observed. Annually, an estimated 200,000 to 400,000 cases of VL are reported worldwide, resulting in approximately 20,000 to 40,000 deaths [1]. These figures are particularly high in countries such as India, Nepal, Bangladesh, and Sudan, according to the World Health Organization (WHO) [2]. Common symptoms of VL, also known as "Kala-azar," include high fever, pallor, weight loss, and splenomegaly [3]. Given the potentially fatal progression of the disease if left untreated, the WHO emphasizes the urgent need for its complete eradication.

Visceral leishmaniasis (VL) is often misdiagnosed as malaria due to overlapping clinical features such as fever and splenomegaly, complicating accurate diagnosis, especially in regions where both diseases are endemic. Additionally, a significant proportion of VL infections remain asymptomatic, posing challenges for disease surveillance and control efforts [4, 5]. Early diagnosis and treatment are crucial for preventing the progression of VL. Current control measures—including the use of insecticide-treated bed nets, indoor residual spraying, and prompt treatment—have effectively reduced morbidity and mortality associated with the disease [6, 7]. However, VL continues to be a public health concern due to factors such as limited access to healthcare, the development of drug resistance, and insecticide resistance in sandfly vectors. Given that individuals who recover from VL typically develop long-lasting immunity, the development of an effective vaccine is considered a promising strategy for disease control. While no human vaccine is currently available, ongoing research and clinical trials are exploring various vaccine candidates to enhance prevention efforts [8].

Mathematical modeling provides a crucial framework for unraveling disease-transmission dynamics, evaluating control measures, and guiding policy decisions. For instance, Dye [9] introduced a deterministic model to describe VL spread in Assam and later refined it to assess various intervention strategies [10]. Since then, numerous authors have developed VL transmission models—Chaves [11], Das [12], Elmojtaba [13], Mubayi [14], Agiyingi [15], and Stauch et al. [1, 6, 16]—yet relatively few validate their structures against fresh epidemiological data. In

regions of Brazil and East Africa, canine VL (CVL) caused by *Leishmania donovani* reaches alarming prevalence among dogs [17], with *Phlebotomus* and *Lutzomyia* sandflies acting as vectors between animal and human hosts [18]. Burattini et al. [19] further expanded this work with an SEIR-type model capturing zoonotic transmission cycles among sandflies, animal reservoirs, and humans. Subsequent studies [1, 6, 13, 16, 20] introduced additional infective stages to account for PKDL development, yet only a handful—Mubayi [14], Stauch et al. [1, 6, 16], and [21]—incorporate validation using new data. Recognizing the limitations of existing diagnostics, recent non-autonomous anthroponotic models stratify populations across humans, dogs, and sandflies [21, 22] but often omit asymptomatic or latent human stages—and, in some cases, overlook the roles of vaccination and reservoir culling in curbing VL transmission [21].

In our current study, we extend the previous model by introducing a latent human class: individuals remain in a latent state for an average of $1/\gamma_e$ days, after which they progress to either an asymptomatic infected compartment (I_A) with probability f_1 or a symptomatic infected compartment (I_H) with probability $1-f_1$. Our primary objectives are to identify the most effective control strategy for reducing transmission and to evaluate the impacts of four interventions: (i) vaccination, (ii) insecticide-treated bed nets, (iii) medical treatment of infected humans, and (iv) culling of infectious reservoirs. In particular, we emphasize the inclusion of vaccination in the model, given its potential as a pivotal measure for suppressing visceral leishmaniasis incidence.

The remainder of the paper is structured as follows. In Section 2, we develop the compartmental model for VL. Section 3 presents its mathematical analysis. In Section 4, we fit the model to monthly incidence data of new VL cases. Section 5 formulates and investigates optimal intervention strategies, and finally, Section 6 showcases the numerical simulation results.

2. MODEL FORMULATION

Following [1, 6, 16], we will formulate a basic SEIR-type model concerning the history of infection to describe the transmission dynamics of VL disease across. The model basically contains human, reservoir and sandfly populations. We have partitioned the total population of humans, $N_H(t)$, into seven specific compartments of subpopulations viz. $S_H, E_H, I_A, I_H, T_H, P_H$ and R_H. That is,

$$N_H(t) = S_H(t) + E_H(t) + I_A(t) + I_H(t) + T_H(t) + P_H(t) + R_H(t).$$

We also partition the populations of reservoir (N_R) and sandfly (N_V) into susceptible reservoir (S_R) and infected reservoir (I_R), and susceptible sandflies (S_V) and infected sandflies (I_V), respectively. Thus,

$$N_R(t) = S_R(t) + I_R(t),\ N_V(t) = S_V(t) + I_V(t).$$

The birth and death rates of susceptible humans (S_H) are Λ_H and μ_h, respectively. Susceptible humans became infectious (i.e., in a latent stage), with $a_0 b\frac{I_V}{N_H}$ being the force of infection where the mean rate of bites per sandfly is denoted by a_0 while the transmission from the sandfly to human (reservoir) is b. After an average period of $\frac{1}{\gamma_e}$ days, latent humans (E_H) became either asymptomatic, I_A, or symptomatic, I_H, with probabilities f_1 and $1-f_1$, respectively. The asymptomatic infected stage usually sustains for $\frac{1}{\gamma_h}$ days. The fraction ρ_1 and ρ_2 of the human population develop symptomatic $KA(I_H)$ and dormant stage (T_H) respectively, and the remaining portion $\rho_3 = 1-\rho_1-\rho_2$ recovers from the asymptomatic infected stage (I_A). Infected humans in the stage (I_H) received treatment at an average rate α_1, and the others die at an average rate δ due to the disease. A proportion of patients σ, from I_H become recovered (R_H), and the remaining part $(1-\sigma)$ of individuals putatively enter the dormant stage (T_H) from which PKDL (P_H) pursues. Humans with PKDL get treated at a normal rate α_2 or recover naturally at an average β. After $\frac{1}{\rho_r}$ days, due to cell resistance, recovered humans (R_H) again turned up to be susceptible S_H. Susceptible reservoirs and sandflies are recruited at a constant rate Λ_R and Λ_V respectively, and attain infection at $a_0 b\frac{I_V}{N_H}$ which is the rate of force of infection and $\mu_1 a_0 c\frac{I_A}{N_H} + a_0 c\frac{I_H}{N_H} + a_0 c\frac{P_H}{N_H} + \mu_2 a_0 c\frac{I_R}{N_R}$ respectively, where c is the probability of transmission for sandfly infection. The natural mortality rates of reservoir and sandflies are μ_r and μ_v, respectively. Keeping these assumptions in mind, we formulate the following system of differential equations:

$$\begin{aligned}
S_H' &= \Lambda_H - a_0 b I_V \frac{S_H}{N_H} - \mu_h S_H + \rho_r R_h,\\
E_H' &= a_0 b I_V \frac{S_H}{N_H} - (\gamma_e + \mu_h) E_H,\\
I_A' &= f_1 \gamma_e E_H - (\gamma_h + \mu_h) I_A,\\
I_H' &= (1-f_1)\gamma_e E_H + \rho_1 \gamma_h I_A - (\alpha_1 + \delta + \mu_h) I_H,\\
T_H' &= (1-\sigma)\alpha_1 I_H - (\delta_p + \mu_h) T_H,\\
P_H' &= \rho_2 \gamma_h I_A + \delta_p T_H - (\alpha_2 + \beta + \mu_h) P_H,\\
R_H' &= \rho_3 \gamma_h I_A + \sigma\alpha_1 I_H + (\alpha_2 + \beta) P_H - \rho_r R_h - \mu_h R_H,\\
S_R' &= \Lambda_R - a_0 b I_V \frac{S_R}{N_R} - \mu_r S_R,\\
I_R' &= a_0 b I_V \frac{S_R}{N_R} - \mu_r I_R,\\
S_V' &= \Lambda_V - S_V(\mu_1 a_0 c\frac{I_A}{N_H} + a_0 c\frac{I_H}{N_H} + a_0 c\frac{P_H}{N_H} + \mu_2 a_0 c\frac{I_R}{N_R} + \mu_v),\\
I_V' &= S_V(\mu_1 a_0 c\frac{I_A}{N_H} + a_0 c\frac{I_H}{N_H} + a_0 c\frac{P_H}{N_H} + \mu_2 a_0 c\frac{I_R}{N_R}) - \mu_v I_V,
\end{aligned} \tag{1}$$

where the total population of humans, reservoir and sandflies which are respectively given by N_H, N_R and N_V will satisfy the following differential equations:

$$\begin{aligned}
N_H' &= \Lambda_H - \mu_h N_H - \delta I_H,\\
N_R' &= \Lambda_R - \mu_r N_R,\\
N_V' &= \Lambda_V - \mu_v N_V.
\end{aligned}$$

2.1. Basic Properties

All parameters of the model (1) are assumed to be nonnegative. Furthermore since the above model monitors living populations, it is assumed that all the state variables are nonnegative at time $t = 0$.

Theorem 1 *Let us consider the initial data as $F(0) \geq 0$, where $F(t) = (S_H(t), E_H(t), I_A(t), I_H(t), T_H(t), P_H(t), R_H(t), S_R(t), I_R(t), S_V(t), I_V(t))$. Then the solutions F(t) of model (1) are nonnegative for all time $t > 0$. Furthermore,*

$$\limsup_{t\to\infty} N_H(t) \leq \frac{\Lambda_H}{\mu_h},$$

$$\limsup_{t\to\infty} N_R(t) \le \frac{\Lambda_R}{\mu_r},$$

$$\limsup_{t\to\infty} N_V(t) \le \frac{\Lambda_V}{\mu_v}.$$

Proof: Please see Appendix A.

Invariant region

The model (1) will be analyzed in a biologically-feasible region as follows. Consider the feasible region

$$\Gamma = \Gamma_H \times \Gamma_R \times \Gamma_V \subset R_+^7 \times R_+^2 \times R_+^2$$

with,

$$\Gamma_H = \{(S_H(t), E_H(t), I_A(t), I_H(t), T_H(t), P_H(t), R_H(t)) : N_H \le \frac{\Lambda_H}{\mu_h}\},$$

$$\Gamma_R = \{(S_R(t), I_R(t)) : N_R \le \frac{\Lambda_R}{\mu_r}\},$$

$$\Gamma_V = \{(S_V(t), I_V(t)) : N_R \le \frac{\Lambda_V}{\mu_v}\}.$$

Theorem 2 *The region $\Gamma = \Gamma_H \times \Gamma_R \times \Gamma_V \subset R_+^7 \times R_+^2 \times R_+^2$ is positively invariant for the basic model (1) with non-negative initial conditions in R_+^{11}.*

Proof: Please see Appendix B.

3. MODEL ANALYSIS

3.1. Disease Free equilibrium and Basic Reproduction number

The disease free equilibrium of the model (1) is given by:

$E_0 = \left(\frac{\Lambda_H}{\mu_h}, 0, 0, 0, 0, 0, 0, \frac{\Lambda_R}{\mu_r}, 0, \frac{\Lambda_V}{\mu_v}, 0\right)$.

Next, we apply the next-generation operator method ([23]) to determine R_0 from system (1).

The basic reproduction number, $\mathcal{R}_0$ is given by $\mathcal{R}_0 = \rho(FV^{-1}) = \mathcal{R}_{0H} + \mathcal{R}_{0R}$ (details can be found in Appendix D),
where, $\mathcal{R}_{0H} = AC$ and $\mathcal{R}_{0R} = BC$,

$$\begin{aligned} A &= a_0 c\gamma_e k_2 [\frac{(\gamma_h+\mu_h)(1-f_1)+f_1\gamma_h\rho_1}{D_n} \\ &\quad + \frac{f_1\mu_1}{(\gamma_e+\mu_h)(\gamma_h+\mu_h)} + \frac{f_1\gamma_h\rho_2(\alpha_1+\delta+\mu_h)}{D_n(\alpha_2+\beta+\mu_h)} \\ &\quad + \frac{(1-\sigma)\alpha_1\delta_p\{(\gamma_h+\mu_h)(1-f_1)+f_1\gamma_h\rho_1\}}{D_n(\alpha_2+\beta+\mu_h)(\delta_p+\mu_h)}], \\ D_n &= (\gamma_e+\mu_h)(\gamma_h+\mu_h)(\alpha_1+\delta+\mu_h), \\ B &= \frac{a_0 c k_2 \mu_2}{k_1 \mu_r}, \; C = \frac{a_0 b}{\mu_v}. \end{aligned}$$

The epidemiological implication of the finding above is that, regardless of the original prevalence of infection, the disease will be eradicated from the population if $R_0 < 1$. The possible interpretation for $\mathcal{R}_{0H}$ and $\mathcal{R}_{0R}$ as the number of secondary infections caused by an infectious sand fly. We note that R_0 is the weighted average of the basic reproduction numbers of reservoir and human populations. The balance of each species' competence to transmit infection weighted by their corresponding population density will determine disease evolution.

Theorem 3 *The disease-free equilibrium is locally asymptotically stable if $\mathcal{R}_0 < 1$ and unstable if $\mathcal{R}_0 > 1$ ([24]).*

3.2. Endemic equilibria

From (1), we get that

$S_H^* = \frac{\Lambda_H}{\mu_h+\theta_H^*(1-F)}$; $E_H^* = \frac{\theta_H^* S_H^*}{l_1}$; $I_A^* = \frac{\theta_H^* S_H^* l_2}{l_1 l_3}$; $I_H^* = \frac{\theta_H^* S_H^*(l_3 l_4+l_2 l_5)}{l_1 l_3 l_6}$;
$T_H^* = \frac{\theta_H^* S_H^*(l_3 l_4+l_2 l_5) l_7}{l_1 l_3 l_6 l_8}$; $P_H^* = \frac{\theta_H^* S_H^*\{(l_3 l_4+l_2 l_5) l_7\delta_p+l_2 l_6 l_8 l_9\}}{l_1 l_3 l_6 l_8 l_{10}}$; $R_H^* = \theta_H^* F$;
$S_R^* = \frac{\Lambda_R}{\mu_r+\theta_R^*}$; $I_R^* = \frac{\Lambda_R\theta_R^*}{(\mu_r+\theta_R^*)\mu_r}$; $S_V^* = \frac{\Lambda_V}{\mu_v+\theta_V^*}$; $I_V^* = \frac{\Lambda_V\theta_V^*}{(\mu_v+\theta_V^*)\mu_v}$;
where $\theta_H^* = \frac{a_0 b I_V^*}{N_H^*}$; $\theta_R^* = \frac{a_0 b I_V^*}{N_R^*}$; $\theta_V^* = \mu_1 a_0 c\frac{I_A^*}{N_H^*} + a_0 c\frac{I_H^*}{N_H^*} + a_0 c\frac{P_H^*}{N_H^*} + \mu_2 a_0 c\frac{I_R^*}{N_R^*}$;
$l_1 = (\gamma_e+\mu_h), l_2 = f_1\gamma_e, l_3 = (\gamma_h+\mu_h), l_4 = (1-f_1)\gamma_e, l_5 = \rho_1\gamma_h, l_6 = (\alpha_1+\delta+\mu_h), l_7 = (1-\sigma)\alpha_1, l_8 = (\delta_p+\mu_h), l_9 = \rho_2\gamma_h, l_{10} = (\alpha_2+\beta+\mu_h), F = \frac{\rho_3\gamma_h I_A^*+\sigma\alpha_1 I_H^*+(\alpha_2+\beta)P_H^*}{\mu_h+\rho_r}$.

Now, $\frac{\theta_H^*}{\theta_R^*} = \frac{N_R^*}{N_H^*}$ implies that $\theta_R^* = \theta_H^* Z(\theta_H^*)$, where $Z(\theta_H^*) = \frac{(\Lambda_H-\delta I_H^*)\mu_r}{\Lambda_R\mu_h}$.

Also, $\theta_V^* = \mu_1 a_0 c\frac{I_A^*}{N_H^*} + a_0 c\frac{I_H^*}{N_H^*} + a_0 c\frac{P_H^*}{N_H^*} + \mu_2 a_0 c\frac{I_R^*}{N_R^*}$;

So, we can write, $\theta_V^* = \frac{\theta_H^* G}{1+H\theta_H^*} + \frac{\mu_2 a_0 c\theta_R^*}{\theta_R^*+\mu_r}$

where, $\theta_H^* G = \mu_1 a_0 c\frac{\theta_H^* S_H^* l_2}{l_1 l_3} + a_0 c\frac{\theta_H^* S_H^*(l_3 l_4+l_2 l_5)}{l_1 l_3 l_6} + a_0 c\frac{\theta_H^* S_H^*\{(l_3 l_4+l_2 l_5) l_7\delta_p+l_2 l_6 l_8 l_9\}}{l_1 l_3 l_6 l_8 l_{10}}$, $N_H^* = S_H^*(1+H\theta_H^*)$.

So, we get, $\theta_V^* = \theta_H^* U(\theta_H^*)$, where, $U(\theta_H^*) = \frac{G}{1+H\theta_H^*} + \frac{\mu_2 a_0 c\theta_H^* Z(\theta_H^*)}{\theta_H^* Z(\theta_H^*)+\mu_r}$.

Substituting I_V^* in θ_V^* and θ_H^* we get,

$$H{\theta_V^*}^2 + \theta_V^* A + B = 0$$

where, $A = H\mu_v + U(\theta_H^*) - (1-F)\frac{\Lambda_V a_0 b}{\Lambda_H\mu_v}$, $B = U(\theta_H^*)(\mu_v - \frac{\Lambda_V a_0 b\mu_h}{\Lambda_H\mu_v})$.

We can obtain the positive equilibrium of the system (1) by solving the above equations. An interesting observation is that if the conditions $B > 0, A < 0$ and $A^2 - 4BH > 0$ hold, then the system has two positive equilibrium points. However, if $B < 0$ or $A^2 - 4BH = 0$ or $B = 0, A < 0$ these conditions hold, then the system (1) tends to have a unique equilibrium point.

3.3. Existence of backward bifurcation

When $R_0 < 1$, we can observe the stable endemic equilibrium point and a stable disease-free equilibrium point exhibiting backward bifurcation. It is interesting to check the similar behaviour for our model (1).

Theorem 4 *The system (1) undergoes backward bifurcation at $R_0 = 1$ whenever the bifurcation coefficient, a, is positive (as $b > 0$ always).*

In order for $R_0 < 1$, the phenomenon of backward bifurcation has serious public health implications; therefore, it is no longer sufficient for effective control (or elimination) of the disease. In this type of a case of (backward bifurcation) situation, the original sizes of the subpopulations compartments of our model (state variables) will determine the effectiveness of disease control or elimination. We will then attempt to determine the value of the bifurcation parameters a & b.

To study the possibility of backward bifurcation, we use the centre manifold theorem ([25, 26]), mainly we use the theorem in Castillo-Chavez and Song ([26]).
For the case when $\mathcal{R}_0 = 1$, and we assume that $a_0 = \phi$ is selected to be the bifurcation parameter, then the Jacobian matrix of the

system (1) at the disease-free equilibrium point is given as follows:

$$\mathcal{J}_\phi = \begin{pmatrix} -\mu_h & 0 & 0 & 0 & 0 & 0 & \rho_r & 0 & 0 & 0 & -y_1 \\ 0 & -y_2 & 0 & 0 & 0 & 0 & 0 & 0 & 0 & 0 & y_1 \\ 0 & y_3 & -y_4 & 0 & 0 & 0 & 0 & 0 & 0 & 0 & 0 \\ 0 & y_5 & y_6 & -y_7 & 0 & 0 & 0 & 0 & 0 & 0 & 0 \\ 0 & 0 & 0 & y_8 & -y_9 & 0 & 0 & 0 & 0 & 0 & 0 \\ 0 & 0 & y_{10} & 0 & \delta_p & -y_{11} & 0 & 0 & 0 & 0 & 0 \\ 0 & 0 & y_{12} & y_{13} & 0 & y_{14} & -y_{15} & 0 & 0 & 0 & 0 \\ 0 & 0 & 0 & 0 & 0 & 0 & 0 & -\mu_r & 0 & 0 & -y_{17} \\ 0 & 0 & 0 & 0 & 0 & 0 & 0 & 0 & -\mu_r & 0 & y_{17} \\ 0 & 0 & -y_{18} & -y_{19} & 0 & -y_{20} & 0 & 0 & -y_{21} & -\mu_v & 0 \\ 0 & 0 & y_{18} & y_{19} & 0 & y_{20} & 0 & 0 & y_{21} & 0 & -\mu_v \end{pmatrix}$$

where, $y_1 = \phi b, y_2 = (\gamma_e + \mu_h), y_3 = f_1\gamma_e, y_4 = (\gamma_h + \mu_h), y_5 = (1 - f_1)\gamma_e, y_6 = \rho_1\gamma_h, y_7 = \alpha_1 + \delta + \mu_h, y_8 = (1 - \sigma)\alpha_1, y_9 = \delta_p + \mu_h, y_{10} = \rho_2\gamma_h, y_{11} = \alpha_2 + \beta + \mu_h, y_{12} = \rho_3\gamma_h, y_{13} = \sigma\alpha_1, y_{14} = \alpha_2 + \beta, y_{15} = (\rho_r + \mu_h), y_{17} = \phi b\frac{N_R^*}{N_H^* + N_R^*}, y_{18} = \mu_1\phi c\frac{N_v^*}{N_H^*}, y_{19} = \phi c\frac{N_v^*}{N_H^*}, y_{20} = \phi c\frac{N_v^*}{N_H^*}, y_{21} = \phi c\mu_2\frac{N_v^*}{N_R^*}, N_v^* = \frac{\Lambda_V}{\mu_v}, N_H^* = \frac{\Lambda_H}{\mu_h}, N_R^* = \frac{\Lambda_R}{\mu_r}$.

Calculation of the eigenvectors of $\mathcal{J}_\phi$: It can be shown that the Jacobin of the system (1) has a right eigenvector given by $W = (w_1, w_2, w_3, w_4, w_5, w_6, w_7, w_8, w_9, w_{10}, w_{11})^T$, where

$$\begin{aligned} w_1 &= \frac{y_1w_{11} - \rho r w_7}{\mu_h} = H_1(w_{11}) \\ w_2 &= \frac{y_1}{y_2}w_{11} \\ w_3 &= \frac{y_3}{y_4}w_2 = H_2(w_{11}) \\ w_4 &= \frac{y_5w_2 + y_6w_3}{y_7} = H_3(w_{11}) \\ w_5 &= \frac{y_8}{y_9}w_4 = H_4(w_{11}) \\ w_6 &= \frac{y_{10}w_3 + \delta_p w_5}{y_{11}} = H_5(w_{11}) \\ w_7 &= \frac{y_{12}w_3 + y_{13}w_4 + y_{14}w_6}{y_{15}} = H_6(w_{11}) \\ w_8 &= \frac{-y_{17}}{\mu_r}w_{11} \\ w_9 &= -w_8 \\ w_{10} &= -w_{11} \\ w_{11} &= \frac{(y_{18}w_3 + y_{19}w_4 + y_{20}w_6 + y_{21}w_9)}{\mu_v} = H_7(w_{11}) \end{aligned} \tag{2}$$

and a left eigenvector given by $V = (v_1, v_2, v_3, v_4, v_5, v_6, v_7, v_8, v_9, v_{10}, v_{11})$, where

$$\begin{aligned} v_1 &= v_7 = v_8 = v_{10} = 0 \\ v_2 &= \frac{y_3v_3 + y_5v_4}{y_2} = G_1(v_{11}) \\ v_3 &= \frac{y_6v_4 + y_{18}v_{11}}{y_4} = G_2(v_{11}) \\ v_4 &= \frac{y_8v_5 + v_{11}y_{19}}{y_7} = G_3(v_{11}) \\ v_5 &= \frac{\delta_p v_6}{y_9} = G_4(v_{11}) \\ v_6 &= \frac{y_{20}}{y_{11}}v_{11} \\ v_9 &= \frac{y_{21}}{\mu_r}v_{11} \\ v_{11} &= v_{11} \end{aligned}$$

Computation of a and b: After some tedious calculations, it can be shown that

$$\begin{aligned} a^* &= X - Y \\ X &= v_{11}w_{10}[\frac{a_0c\mu_1w_3 + a_0cw_4 + a_0cw_6}{N_H^*} + \frac{a_0c\mu_2w_9}{N_R^*}] \\ Y &= v_{11}(\sum_{i=1}^{7} w_i)\frac{a_0cN_v^*}{(N_H^*)^2}(w_3\mu_1 + w_4 + w_6) + v_2w_{11}\frac{a_0b}{N_H^*}(\sum_{i=2}^{7} w_i) \\ &\quad + v_{11}w_9\mu_2\frac{a_0cN_v^*(w_8 + w_9)}{(N_R^*)^2} + v_9w_{11}w_9\frac{a_0b}{N_R^*} \end{aligned}$$

and

$$\begin{aligned} b^* &= b(v_2w_{11} + +v_9w_{11}) \\ &\quad + cv_{11}[(w_3\mu_1 + w_4 + w_6)\frac{N_v^*}{N_H^*} + \mu_2w_9]\frac{N_v^*}{N_R^*} \end{aligned}$$

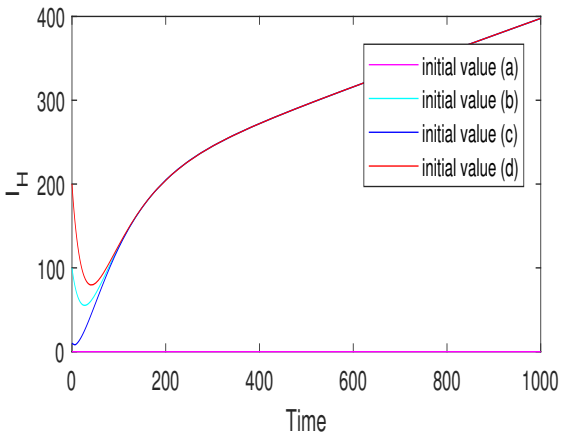

Figure 1. Existence of backward bifurcation for the model (1).

Figure (1) confirms the presence of backward bifurcation in the model (1). Figure (1) shows a time-series plot with different initial conditions convergent to both the disease-free equilibrium (DFE) and an endemic equilibrium point (EEP) when $R_0 = 0.88 < 1$. The initial values with $I_H(0) > 0$ converges to endemic equilibrium point (EEP), otherwise it will converge to the disease-free equilibrium (DFE). Parameter values used are : $\Pi_h = 160, \mu_h = 0.002, \rho_r = 0.25, \rho_2 = .001, \alpha_1 = 0.03, \gamma_h = 0.02, \sigma = 0.84, f_1 = 0.98, b = 0.40, \rho_1 = 0.002, \rho_3 = 1 - \rho_1 - \rho_2, k_1 = 0.60, k_2 = 2, c = 0.07, \gamma_e = 0.01, \mu_v = 0.06, \Pi_v = 200, \Pi_r = 75, \delta_p = 0.0016, \delta = 0.011, \alpha_2 = 0.006, \beta = .002, \mu_2 = 1, \mu_1 = 1, \mu_r = 0.065$.

4. MODEL CALIBRATION

In this subsection, first, the author calibrates the model (1) to yearly incidence data of Visceral Leishmaniasis in South Sudan ([27]). The estimated parameters are $b, f1, k1, k2$, and c. (Refer to the Appendix E section for more details).

Figure (2) illustrates the fitting of the model (1) for the cumulative reported new VL cases. Tables 1 and 2 consist of the values of the estimated model parameters. In South Sudan, observing the estimated initial values of various infected human compartments (see Table 2) reveals that the epidemic was already widespread among the population when the data were obtained (January 2011). With a 95% confidence interval,

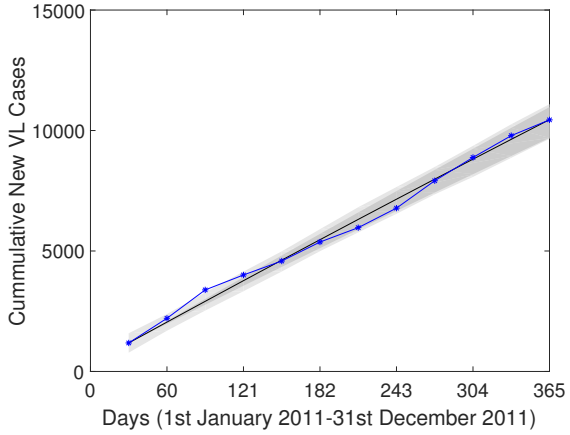

Figure 2. Plots of the observed cumulative data and the out put of the fitted model (1). Cumulative new VL cases (blue star) from the data, and model simulated data (thick black curve) are plotted with the parameter estimates using parameter values and initial conditions from Table 1 and Table 2 for the time period (1st January 2011 - 31st December 2011).

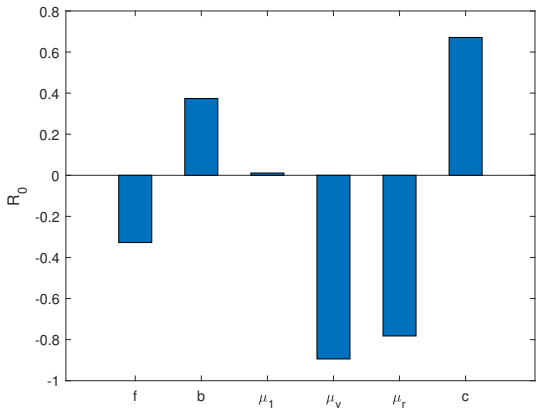

Figure 3. Plot of the PRCC over time of the model (1). The PRCC is calculated with respect to R_0 with significant level 0.05, using 10000 samples.

the estimated value of transmission probability that accounts for human susceptibility to infection is 0.20 on average. The primary reproduction number's estimated value is 3.91 (with a 95% confidence interval).

4.1. Sensitivity analysis

Latin Hypercube Sampling (LHS) method in combination with Partial Rank Correlation Coefficient (PRCC) multivariate analysis ([28], [29], [30]) were used to do the sensitivity analysis for the model (1) on 2000 random parameter samples. A useful method for predicting the nonlinear but monotonic connection between input and model result is PRCC. The estimated parameters in Section (4) serve as the inputs. The parameters' minimum and maximum values are shown in Table 2. When determining the value of R_0, the most crucial parameters are b, f, μ_r, c, and μ_v (See Figure (3)). A positive value of the PRCC score implies that increasing that particular parameter will increase the value of R_0. In contrast, a negative value shows that decreasing that parameter R_0 also tends to decline.

Table 1. Parameter description, values, posterior summary and sources of model (1).

Para.	Description	Value	Range	Source
Λ_H	Constant recruitment rate of Human	$\mu_H N_H(0)$ day^{-1}	–	[21]
μ_H	Death rate of Human	5.64×10^{-5} day^{-1}	–	[31]
Λ_R	Constant recruitment rate of Reservoir	$\mu_R N_R(0)$ day^{-1}	–	[6]
μ_R	Death rate of Reservoir	0.0017 day^{-1}	–	[10]
Λ_V	Constant recruitment rate of Sandfly	$\mu_V N_V(0)$ day^{-1}	–	[6]
μ_V	Death rate of Sandfly	0.0668 day^{-1}	–	[6]
δ	Death rate due to VL	0.011 day^{-1}	–	[32]
$1/\delta_p$	Duration until relapse to PKDL stage	630 days	–	[6]
α_2	Treatment rate in PKDL stage	0.033 day^{-1}	–	[33]
β	Natural recovery rate from PKDL stage	0.002 day^{-1}	–	[34]
$1/\rho_r$	Period before recovered humans becoming susceptible again	0.0032 day^{-1}	–	[6]
ρ_1	Fraction developing symptomatic KA	0.01	[0.01, 0.02]	[6]
ρ_2	Fraction developing PKDL	10^{-4}	$[10^{-4}, 2 \times 10^{-4}]$	[6]
ρ_3	Fraction recovering	$1-\rho_1-\rho_2$	–	–
σ	Proportion moving from KA to recovery	0.84	[0.80, 0.90]	[6]
μ_2	Infection probability of sandfly biting reservoir	1	–	Assumed
a_0	Average biting rate of sandflies	0.20 day^{-1}	[0.15, 0.3]	[6]
α_1	Treatment rate of VL in symptomatic KA stage	0.03 day^{-1}	[0.01, 0.04]	[6]
$1/\gamma_e$	Sojourn time in the exposed class	0.01526 day^{-1}	[0.01, 0.025]	[6]
$1/\gamma_h$	Sojourn time in the asymptomatic KA stage	0.068 day^{-1}	[0.01, 0.02]	[6]
b	Transmission probability in human and reservoir	0.205	[0.12, 0.40]	Estimated
f_1	Fraction of exposed humans developing asymptomatic KA	0.92	[0.85, 0.99]	Estimated
c	Transmission probability in sandfly population	0.07	[0.01, 0.2]	Estimated
k_1	Reservoir per human	0.60	[0.4, 1]	Estimated
k_2	Sandfly per human	1.25	[0.6, 2]	Estimated
R_0	Basic reproduction number	3.91	–	Estimated

5. THE OPTIMAL CONTROL PROBLEM

Some intervention strategies, like the use of treated bed nets, vaccination of the human population, the effective treatment of infected persons with antibiotics, and the culling of reservoirs, are some measures the author includes in this section to decrease the spread of visceral leishmaniasis infection. We should include vaccination as a control technique in VL mathematical modelling since it can be employed as a crucial strategy to lower the prevalence of VL. The control functions that we have used here are, u_1, u_2, u_3, u_4 and u_5, which respectively represent time-dependent efforts of bednets, vaccination, treatment of symptomatic KA patients, treatment of PKDL patients and culling of reservoirs. The controls are practised over a time interval of $[0; t_f]$.

System of nonlinear differential equations representing the effect of different interventions on the basic model (1), is given as follows:

$$\begin{aligned}
S_H' &= \Lambda_H - a_0 b I_V \frac{S_H}{N_H}(1-u_1(t)) - \mu_h S_H + \rho_r R_h - u_2\sigma_2 S_H \\
E_H' &= a_0 b I_V \frac{S_H}{N_H}(1-u_1(t)) - (\gamma_e + \mu_h)E_H \\
I_A' &= f_1\gamma_e E_H - (\gamma_h + \mu_h)I_A \\
I_H' &= (1-f_1)\gamma_e E_H + \rho_1\gamma_h I_A - (u_3(t) + \delta + \mu_h)I_H \\
T_H' &= (1-\sigma)u_3(t)I_H - (\delta_p + \mu_h)T_H \\
P_H' &= \rho_2\gamma_h I_A + \delta_p T_H - (u_4(t) + \beta + \mu_h)P_H \\
R_H' &= \rho_3\gamma_h I_A + \sigma u_3(t)I_H + (u_4(t)+\beta)P_H + u_2\sigma_2 S_H \\
&\quad -\rho_r R_h - \mu_h R_H \\
S_R' &= \Lambda_R - a_0 b I_V \frac{S_R}{N_R} - (\mu_r + u_5(t))S_R \qquad (3) \\
I_R' &= a_0 b I_V \frac{S_R}{N_R} - (\mu_r + u_5(t))I_R \\
S_V' &= \Lambda_V - (\mu_1 a_0 c S_V \frac{I_A}{N_H} + a_0 c S_V \frac{I_H}{N_H} + a_0 c S_V \frac{P_H}{N_H})(1-u_1(t)) \\
&\quad -\mu_2 a_0 c S_V \frac{I_R}{N_R} - \mu_v S_V \\
I_V' &= (\mu_1 a_0 c S_V \frac{I_A}{N_H} + a_0 c S_V \frac{I_H}{N_H} + a_0 c S_V \frac{P_H}{N_H})(1-u_1(t)) \\
&\quad +\mu_2 a_0 c S_V \frac{I_R}{N_R} - \mu_v I_V
\end{aligned}$$

The initial conditions being $S_H(0)$, $E_H(0)$, $I_A(0)$, $I_H(0)$, $T_H(0)$, $P_H(0)$, $R_H(0)$, $S_R(0)$, $I_R(0)$, $S_V(0)$, $I_V(0)$ and the above model parameters are listed in **Table 1** and **Table 2** . The controls $u_1(t), u_2(t), u_3(t), u_4(t)$ and $u_5(t)$ for our model are bounded and Lebesgue integrable functions.

The control problem involves minimizing the number of infected individuals with Visceral leishmaniasis subject to the system (3). The objective function for our model that has to be minimized is defined in the following manner:

$$J(u_1,u_2,\cdots,u_5) = \int_0^{t_f} (A_1 I_A(t) + A_2 I_H(t) + A_3 P_H(t) + A_4 I_R(t) + \tfrac{1}{2}Bu_1^2 + \tfrac{1}{2}Cu_2^2 + \tfrac{1}{2}Du_3^2 + \tfrac{1}{2}Eu_4^2 + \tfrac{1}{2}Fu_5^2)dt;$$

subject to the state equation (3).

Here t_f is the final time and A_1, A_2, A_3 and A_4 are weight constants of the I_A, I_H, P_H, I_R group, respectively. In contrast, B, C, D, E, and F are weight constants for bed nets, vaccination, treatment (for I_H, P_H) and culling efforts, respectively, which regularize the optimal control. We assume no linear relationship exists between these interventions' coverage and their corresponding costs. The weight constants play a significant role in balancing the infectious individuals and cost terms according to their size and importance. These weight constants might be different for different countries or scenarios. We choose the baseline weight constants as Table (3) for simplicity.

The author searches for the optimal controls $u_1^*(t)$, $u_2^*(t)$, $u_3^*(t)$, $u_4^*(t)$ and $u_5^*(t)$ such that

$$J(u_1^*, u_2^*, \cdots, u_5^*) = \min\{J(u_1,u_2,\cdots,u_5); (u_1,u_2,\cdots,u_5) \in U\}$$

where $U = \{(u_1(t), u_2(t), \cdots, u_5(t)); (u_1(t), u_2(t), \cdots, u_5(t))$ measurable, $a_i \le u_i(t) \le b_i, i = 1,2,3,4,5, t \in [0, t_f]\}$ is the control set.

Table 2. Demographic parameters description, values and posterior summary.

Demog. Param.	Description	Lower	Upper	Source/ value
$N_H(0)$	Total human population	1.05×10^7	1.05×10^7	[31]
$S_H(0)$	Susceptible humans	$0.80N_H(0)$	$0.90N_H(0)$	8.15×10^6
$E_H(0)$	Latent humans	$0.085N_H(0)$	$0.10N_H(0)$	8.75×10^5
$I_H(0)$	Symptomatic KA	$0.80C(0)$	$0.88C(0)$	1040
$P_H(0)$	PKDL population	$0.08C(0)$	$0.12C(0)$	96
$R_H(0)$	Immune humans	$0.08N_H(0)$	$0.10N_H(0)$	9.10×10^5
$I_V(0)$	Infected sandflies	0	$0.0002N_V(0)$	1790
$I_R(0)$	Infected reservoirs	0	$0.0004N_R(0)$	1250

Table 3. Computational parameters values

Comp. parameter	Symbol	Value	Source
Final time	t_f	100 days	Assumed
Upper bound u_1	b_1	1	Assumed
Lower bound u_1	a_1	0	Assumed
Upper bound u_2	b_2	1	Assumed
Lower bound u_2	a_2	0	Assumed
Upper bound u_3	b_3	1	Assumed
Lower bound u_3	a_3	0	Assumed
Upper bound u_4	b_4	1	Assumed
Lower bound u_4	a_4	0	Assumed
Upper bound u_5	b_5	1	Assumed
Lower bound u_5	a_5	0	Assumed
Weight u_1	B	1	Assumed
Weight u_2	C	1	Assumed
Weight u_3	D	1	Assumed
Weight u_4	E	1	Assumed
Weight u_5	F	1	Assumed

5.1. Analysis of the Optimal Control Problem

The conditions that an optimal control must satisfy come from Pontryagin's Maximum Principle. The Hamiltonian H, with respect to u_1, u_2, u_3, u_4 and u_5 can be written as:

$$\begin{aligned}
H &= (A_1 I_A(t) + A_2 I_H(t) + A_3 P_H(t) + A_4 I_R(t) + \frac{1}{2}Bu_1^2 + \frac{1}{2}Cu_2^2 \\
&+ \frac{1}{2}Du_3^2 + \frac{1}{2}Eu_4^2 + \frac{1}{2}Fu_5^2) + \sum_{i=1}^{11}\lambda_i g_i \qquad (4)
\end{aligned}$$

where g_i is the right-hand side of the differential equation of the i^{th} state variable and λ_i are the adjoint variables. By applying Pontryagin's Maximum Principle, one can get the following result:

Proposition 1. *An optimal control exists given by,* u_1^*, u_2^*, u_3^*, u_4^* *and* u_5^* *and corresponding solution,* S_H^*,E_H^*, I_A^*, I_H^*, T_H^*, P_H^*, R_H^*, S_R^*, I_R^*, S_V^* *and* I_V^*, *that minimizes the objective function* $J(u_1,u_2,u_3,u_4,u_5)$ *over U. Furthermore, there exist adjoint functions,* $\lambda_1(t),\lambda_2(t),...,\lambda_{11}(t)$ *such that:*

$$\begin{aligned}
\frac{\partial\lambda_1}{\partial t} &= (a_0 b\frac{I_V}{N_H}(1-u_1(t))(1-\frac{S_H}{N_H}))(\lambda_1-\lambda_2)+\mu_h\lambda_1+u_2\sigma_2(\lambda_1-\lambda_7)\\
&\quad -(\lambda_{10}-\lambda_{11})(1-u_1(t))(\mu_1 a_0 c S_V\frac{I_A}{{N_H}^2}+a_0 c S_V\frac{I_H}{{N_H}^2}+a_0 c S_V\frac{P_H}{{N_H}^2})\\
\frac{\partial\lambda_2}{\partial t} &= \lambda_2(\mu_h+\gamma_e)-a_0 b\frac{I_V S_H}{{N_H}^2}(1-u_1(t))(\lambda_1-\lambda_2)-\gamma_e(f_1\lambda_3+(1-f_1)\lambda_4)\\
&\quad -(\lambda_{10}-\lambda_{11})(1-u_1(t))(\mu_1 a_0 c S_V\frac{I_A}{{N_H}^2}+a_0 c S_V\frac{I_H}{{N_H}^2}+a_0 c S_V\frac{P_H}{{N_H}^2})\\
\frac{\partial\lambda_3}{\partial t} &= -A_1+\lambda_3(\mu_h+\gamma_h)-\gamma_h(\rho_1\lambda_4+\rho_2\lambda_5+\rho_3\lambda_6)+(\mu_1 a_0 c\frac{S_V}{N_H}(\lambda_{10}-\lambda_{11})(1-u_1(t)))\\
&\quad -(\lambda_{10}-\lambda_{11})(1-u_1(t))(\mu_1 a_0 c S_V\frac{I_A}{{N_H}^2}+a_0 c S_V\frac{I_H}{{N_H}^2}+a_0 c S_V\frac{P_H}{{N_H}^2})\\
&\quad -a_0 b\frac{I_V S_H}{{N_H}^2}(1-u_1(t))(\lambda_1-\lambda_2)\\
\frac{\partial\lambda_4}{\partial t} &= -A_2+(u_3(t)+\mu_h+\delta)\lambda_4-u_3(t)((1-\sigma)\lambda_5+\sigma\lambda_7)+a_0 c\frac{S_V}{N_H}(\lambda_{10}-\lambda_{11})(1-u_1(t))\\
&\quad -(\lambda_{10}-\lambda_{11})(1-u_1(t))(\mu_1 a_0 c S_V\frac{I_A}{{N_H}^2}+a_0 c S_V\frac{I_H}{{N_H}^2}+a_0 c S_V\frac{P_H}{{N_H}^2})\\
&\quad -a_0 b\frac{I_V S_H}{{N_H}^2}(1-u_1(t))(\lambda_1-\lambda_2)\\
\frac{\partial\lambda_5}{\partial t} &= (\delta_p+\mu_h)\lambda_5-\delta_p\lambda_6-(\lambda_{10}-\lambda_{11})(1-u_1(t))(\mu_1 a_0 c S_V\frac{I_A}{{N_H}^2}\\
&\quad +a_0 c S_V\frac{I_H}{{N_H}^2}+a_0 c S_V\frac{P_H}{{N_H}^2})-a_0 b\frac{I_V S_H}{{N_H}^2}(1-u_1(t))(\lambda_1-\lambda_2)\\
\frac{\partial\lambda_6}{\partial t} &= -A_3+(u_4(t)+\beta+\mu_h)\lambda_6-(u_4(t)+\beta)\lambda_7+a_0 c\frac{S_V}{N_H}(\lambda_{10}-\lambda_{11})(1-u_1(t))\\
&\quad -(\lambda_{10}-\lambda_{11})(1-u_1(t))(\mu_1 a_0 c S_V\frac{I_A}{{N_H}^2}+a_0 c S_V\frac{I_H}{{N_H}^2}+a_0 c S_V\frac{P_H}{{N_H}^2})\\
&\quad -a_0 b\frac{I_V S_H}{{N_H}^2}(1-u_1(t))(\lambda_1-\lambda_2)\\
\frac{\partial\lambda_7}{\partial t} &= (\mu_h+\rho_r)\lambda_7-\rho_r\lambda_1-(\lambda_{10}-\lambda_{11})(1-u_1(t))(\mu_1 a_0 c S_V\frac{I_A}{{N_H}^2}\\
&\quad +a_0 c S_V\frac{I_H}{{N_H}^2}+a_0 c S_V\frac{P_H}{{N_H}^2})-a_0 b\frac{I_V S_H}{{N_H}^2}(1-u_1(t))(\lambda_1-\lambda_2)\\
\frac{\partial\lambda_8}{\partial t} &= a_0 b\frac{I_V}{N_R}(1-\frac{S_R}{N_R})(\lambda_8-\lambda_9)+(\mu_r+u_5(t))\lambda_8-\mu_2 a_0 c\frac{S_V I_R}{{N_R}^2}(\lambda_{10}-\lambda_{11})\\
\frac{\partial\lambda_9}{\partial t} &= -A_4+(\mu_r+u_5(t))\lambda_9-a_0 b\frac{I_V S_R}{{N_R}^2}(\lambda_8-\lambda_9)-\mu_2 a_0 c\frac{S_V I_R}{{N_R}^2}(\lambda_{10}-\lambda_{11})\\
&\quad +\mu_2 a_0 c\frac{S_V}{N_R}(\lambda_{10}-\lambda_{11})\\
\frac{\partial\lambda_{10}}{\partial t} &= \{(\mu_1 a_0 c\frac{I_A}{N_H}+a_0 c\frac{P_H}{N_H}+a_0 c\frac{I_H}{N_H})(1-u_1(t))+\mu_2 a_0 c\frac{I_R}{N_R}\}(\lambda_{10}-\lambda_{11})+(\mu_v)\lambda_{10}\\
\frac{\partial\lambda_{11}}{\partial t} &= a_0 b\frac{S_H}{N_H}(1-u_1(t))(\lambda_1-\lambda_2)+a_0 b\frac{S_R}{N_R}(\lambda_8-\lambda_9)+(\mu_v)\lambda_{11} \qquad (5)
\end{aligned}$$

with transversality conditions

$$\lambda_i(t_f)=0, i=1,2,...,11. \qquad (6)$$

$$\begin{aligned}
u_1^* &= \min\left\{b_1,\max\left[a_1,\frac{(\lambda_2-\lambda_1)a_0 b I_V S_H+N_H U_n}{N_H B}\right]\right\}\\
u_2^* &= \min\left\{b_2,\max\left[a_2,\frac{(\lambda_1-\lambda_7)\sigma_2 S_H}{C}\right]\right\}\\
u_3^* &= \min\left\{b_3,\max\left[a_3,\frac{(\lambda_4-(1-\sigma)\lambda_5-\sigma\lambda_7)I_H}{D}\right]\right\}\\
u_4^* &= \min\left\{b_4,\max\left[a_4,\frac{(\lambda_6-\lambda_7)P_H}{E}\right]\right\}\\
u_5^* &= \min\left\{b_5,\max\left[a_5,\frac{(\lambda_8 S_R+\lambda_9 I_R)}{F}\right]\right\}
\end{aligned}$$

where $U_N=(\mu_1 a_0 c\frac{I_A S_V}{N_H}+a_0 c\frac{P_H S_V}{N_H}+a_0 c\frac{I_H S_V}{N_H})(\lambda_{11}-\lambda_{10})$.

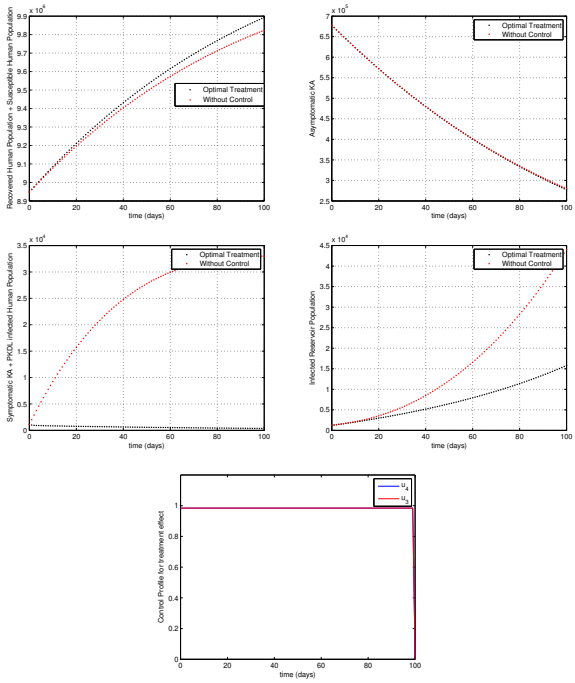

Figure 4. Optimal solutions for the model (3) showing the effect of the optimal treatment.

6. NUMERICAL SIMULATION

In the following section, the author discusses the simulation results for the optimal control of different parameters. The values for the parameters used are given in **Table 1, Table 2**, and the other computational parameters are given in **Table 3**.

The author considers five scenarios: optimal treatment control, optimal vaccination control, optimal treated bed net policy, optimal culling policy, and all the controls as first, second, third, fourth, and fifth, respectively.

We observe the following scenario:

6.1. First scenario

With this strategy, only treatment u_3u_4 has been employed to optimize the objective function J. The sum of susceptible with the recovered population (S_H+R_H) increases (Figure (4)(a)) and asymptomatic KA (I_A) (Figure (4)(b)), symptomatic KA+ PKDL (I_H+P_H) (Figure (4)(c)), infected reservoirs (I_R) (Figure (4)(d)) decreases significantly. At $t=100$ days, the differences between optimal treatment control and no control for S_H+R_H, I_A, I_H+PKDL and I_R are respectively 0.8×10^6; 0.9×10^5; $3.2\times10^4 and 2.8\times10^4$ (see Figure (4)). According to the control profile depicted in Figure (4)(e), we can conclude that the control u_3u_4 should be at a maximum level for 98 days. This strategy suggests optimal preventive strategies against VL in a community. At the same time, an adequate treatment regime is not put in place simultaneously and would not be a practical approach to control the disease at the final time.

6.2. Second scenario

With this scenario, only vaccination u_2 is used to optimize the objective function J. The infected human and reservoir population dynamics do not tend to exhibit any significant effect under the use of this control strategy. We can observe this in (Figure (5)(c) and

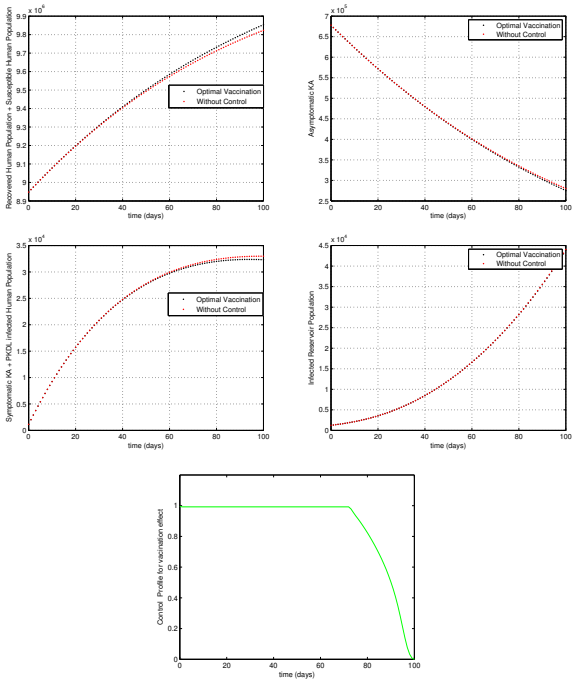

Figure 5. Optimal solutions for the model (3) showing the effect of the optimal vaccination.

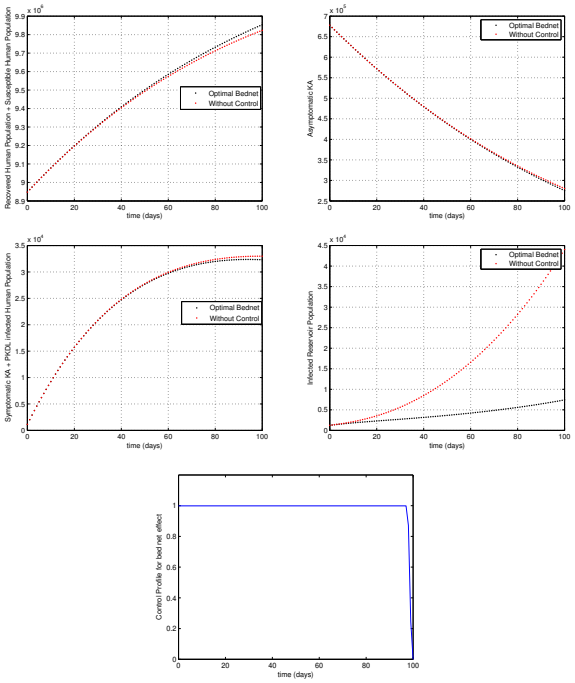

Figure 6. Optimal solutions for the model (3) showing the effect of the optimal treated bednet.

(d)). This may be connected to the fact that treatment of infected individuals is neglected, and as a result, the disease persists in the community. However, a notable fact lies in the inference that on employing this control mechanism, the Susceptible + Reservoir population increases by 0.5×10^6 (Figure (5)(a)) and asymptomatic KA (I_A) infected population decreases (Figure (5)(b)). The optimal vaccination profile is displayed in Figure (5)(e), where we can observe that for 72 days, the optimal vaccination policy is 100%. This scenario suggests that high levels of vaccine efficacy would be required to reduce the equilibrium prevalence of VL significantly. Vaccination rates impact the transient dynamics through the rate of reduction of cases but ultimately have little role in long-term prevalence where new cases are continuously imported.

6.3. Third scenario

The author considers only bed net control u_1 in the third scenario. It can be observed in Figure (6)(a), (b), (c) and (d) that $S_H + R_H$ increase, I_A, $I_H + PKDL$ and I_R decreases significantly. Figure (6)(e) shows the optimal treated bed net policy profile. To decrease VL infection, bed net should be used at 100% intensively for almost 100 days.

6.4. Fourth scenario

Here, we employ the optimal culling effect u_5 for optimization of the objective function J while keeping the other controls at a constant value of zero. Small differences can be observed for $S_H + R_H$ (Figure (7)(a)), Asymptomatic humans (Figure (7)(b)) and I_H+ PKDL (Figure (7)(c)) cases but u_5 can eliminate the infected reservoirs from the society (Figure (7)(d)). Figure (7)(e) depicts that u_5 should be at around 100% for the first 12 days before dropping slowly to the lower bound on the 99th day. This shows that the effective and optimal use of the culling effect on the reservoirs in controlling VL does not benefit the community in the long run.

6.5. Fifth scenario

This approach aims to optimize the objective function J by implementing all available control measures. As shown in Figure (8), the application of the control strategy leads to a consistent decline in all infected compartments over time, whereas in the absence of controls, infection levels increase. The strategy also effectively reduces the number of asymptomatic human cases. The treatment controls (u_3 and u_4) remain at 100% effectiveness for the majority of the period. In comparison, the usage of bed nets (u_2) and vaccination (u_1) begins at 100% but steadily declines to their minimum levels within 98 days. Meanwhile, the culling control (u_5) starts at approximately 22% and gradually decreases to its lower bound by day 99. This suggests that, under the optimal strategy, the culling of reservoirs requires relatively minimal effort.

7. CONCLUSION

Authors of [21] discussed a general non-autonomous anthroponotic visceral leishmaniasis model that considers the human (infected compartments divided into symptomatic, asymptomatic, PKDL-infected classes) dog and sand fly populations and probes further to investigate the efficacy of various control strategies. However, in this article, we modified their model as humans stay latent for an average period of $\frac{1}{\gamma_e}$ days, and became either asymptomatic, I_A, or symptomatic, I_H, with probabilities f_1 and $1 - f_1$, respectively. We mathematically analysed the model to derive the basic reproduction number R_0, and estimated the value for the year 2011. Visceral leishmaniasis or Kala-Azar is one of the most severely neglected tropical diseases perceived by the World Health Organization (WHO). The danger of this debilitating disease persists due to the inaccessibility of promising treatment or human immunization. Broad research is going on to build up a promising vaccine to prevent this

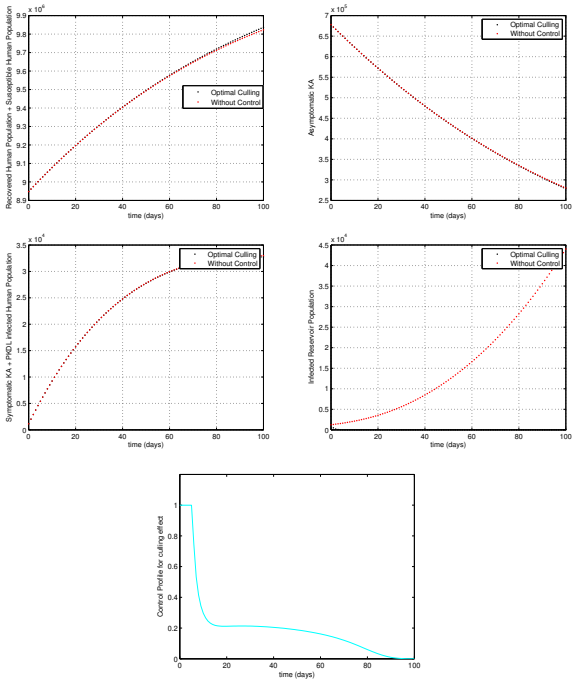

Figure 7. Optimal solutions for the model (3) showing the effect of the optimal culling effect.

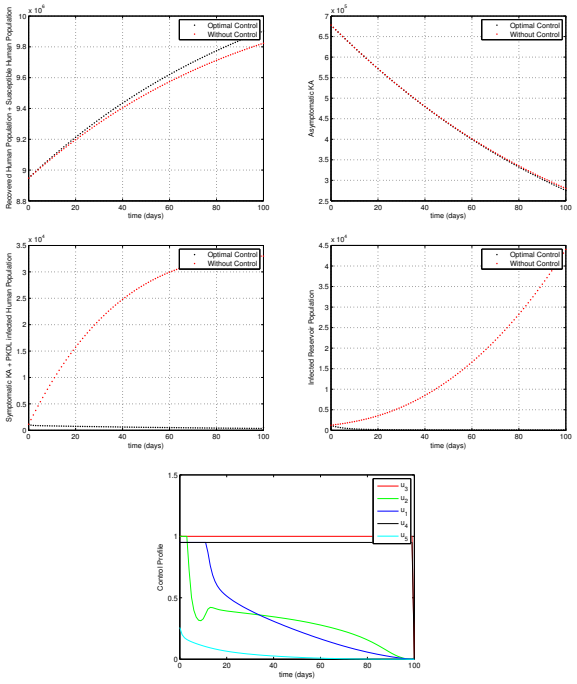

Figure 8. Optimal solutions for the model (3) showing the effect of the optimal control policy.

devastating disease [35, 36]. The significant job can be played by vaccination for preventing the span of the disease. In this article, we considered four types of control, i.e., use of treated bednets, vaccination, treatment of infective, and culling effect of reservoirs (authors of [21] did not consider vaccination and culling effect) to discuss the optimal use of control scenarios. Optimal control policy proposes that combining the mass treatment, vaccination, bed net, and culling effect give superior and productive outcomes for diminishing VL prevalence. However, we find that mass treatment is vital instead of other prevention strategies during the outbreak of VL, and the optimal use of only culling effect to the reservoirs is not beneficial to the society for the control of VL.

8. CONFLICT OF INTEREST

On behalf of all authors, the corresponding author states that there is no conflict of interest.

9. DATA AVAILABILITY STATEMENT

The data sets generated during and/or analyzed during the current study are available from the corresponding author on reasonable request.

10. APPENDICES

10.1. Appendix A. Proof of Theorem 1

Following the frame work of ([37]), let $t_1 = \sup\{t > 0 : F(t) > 0\}$. From the 1st equation of the model (1), we get that

$$S_H' \geq \Lambda_H - \Lambda(I_V, N_H)S_H - \mu_h S_H$$

which can be rewritten as

$$\frac{d}{dt}\{S_H(t)exp[\int_0^{t_1} \Lambda(I_V, N_H)du + \mu_h(t)]\}$$
$$\geq \Lambda_H exp[\int_0^{t_1} +\Lambda(I_V, N_H)du + \mu_h(t)]$$

So that,

$$S_H(t_1)exp[\int_0^{t_1} \Lambda(I_V, N_H)du + \mu_h(t)] - S_H(0)$$
$$\geq \Lambda_H exp[\int_0^{t_1} +\Lambda(I_V, N_H)du + \mu_h(t)].$$

Hence, $S_H(t_1) > 0$.
Similarly it can be shown that $F > 0$ if $t_1 > 0$.
Next, we observe that $0 < S_H(t) \leq N_H(t), 0 < E_H(t) \leq N_H(t), 0 < I_A(t) \leq N_H(t), 0 < I_H(t) \leq N_H(t), 0 < T_H(t) \leq N_H(t), 0 < P_H(t) \leq N_H(t), 0 < R_H(t) \leq N_H(t)$. Now,

$$N_H' = \Lambda_H - \mu_h N_H - \delta I_H$$

Thus,

$$\Lambda_H - \mu_h N_H \geq N_H' \geq \Lambda_H - (\mu_h + \delta)N_H.$$

Hence,

$$\frac{\Lambda_H}{(\mu_h + \delta)} \leq \liminf_{t\to\infty} N_H(t) \leq \limsup_{t\to\infty} N_H(t) \leq \frac{\Lambda_H}{\mu_h},$$

as required. Similarly,

$$\frac{\Lambda_R}{(\mu_r)} \leq \liminf_{t\to\infty} N_R(t) \leq \limsup_{t\to\infty} N_R(t) \leq \frac{\Lambda_R}{\mu_r},$$

and

$$\frac{\Lambda_V}{(\mu_v)} \leq \liminf_{t\to\infty} N_V(t) \leq \limsup_{t\to\infty} N_V(t) \leq \frac{\Lambda_V}{\mu_v}.$$

10.2. Appendix B. Proof of Theorem 2

We observe that,

$$\begin{aligned} N'_H &= \Lambda_H - \mu_h N_H - \delta I_H \\ N'_R &= \Lambda_R - \mu_r N_R \\ N'_V &= \Lambda_V - \mu_v N_V \end{aligned}$$

Using standard comparison theorem, it can be shown that $N_H(t) \leq N_H(0)e^{-\mu_h t} + (1-\mu_h t)\frac{\Lambda_H}{\mu_h}$, in particular $N_H(t) \leq \frac{\Lambda_H}{\mu_h}$ if $N_H(0) \leq \frac{\Lambda_H}{\mu_h}$.

Similarly, $N_R(t) \leq N_R(0)e^{-\mu_r t} + (1-\mu_r t)\frac{\Lambda_R}{\mu_r}$, in particular $N_R(t) \leq \frac{\Lambda_R}{\mu_r}$ if $N_R(0) \leq \frac{\Lambda_R}{\mu_r}$ and

$N_V(t) \leq N_V(0)e^{-\mu_v t} + (1-\mu_v t)\frac{\Lambda_V}{\mu_v}$, in particular $N_V(t) \leq \frac{\Lambda_V}{\mu_v}$ if $N_V(0) \leq \frac{\Lambda_V}{\mu_v}$.

Thus, the region Γ is positively invariant. Hence, it is sufficient to consider the dynamics of the flow generated by (1) in Γ. In this region, the model is epidemiologically and mathematically well-posed. Thus, every solution of the model (1) with initial conditions in Γ remains in Γ for all $t > 0$. Therefore, the Γ-limit sets of the system (1) are contained in Γ.

10.3. Appendix C. Proof of Theorem 3

Using Theorem (3) in [38], we can rewrite the system (1) in the form

$$\begin{aligned} \frac{dX}{dt} &= F(X,Z) \\ \frac{dZ}{dt} &= G(X,Z), \qquad G(X,0) = 0 \end{aligned} \tag{7}$$

where the components of the column-vector $X \in R^m$ denotes the number of uninfected individuals and the components of vector $Z \in R^n$ denote the number of infected individuals.
For the system (1),

$$\begin{aligned} X &= (S_H, R_H, S_R, S_V) \\ Z &= (E_H, I_A, I_H, T_H, P_H, I_R, I_V) \\ F(X,0) &= (\Lambda_H - \mu_h S_H + \rho_r R_H,\ -(\rho_r + \mu_h)R_H, \\ &\quad \Lambda_R - \mu_r S_R,\ \Lambda_V - \mu_v S_V)^T \end{aligned} \tag{8}$$

$$\mathbf{A} = -\mathbf{V}$$

And the column-vector $\hat{G}(X,Z)$ is given by

$$\begin{aligned} \hat{G}(X,Z) = \Bigg(& a_0 b I_V \left(1 - \frac{S_H}{N_H}\right) \quad 0 \quad 0 \quad 0 \quad a_0 b I_V \left(1 - \frac{S_R}{N_R}\right) \\ & \mu_1 a_0 c I_A \left(1 - \frac{S_V}{N_H}\right) + a_0 c (I_H + P_H)\left(1 - \frac{S_V}{N_H}\right) \\ & + \mu_2 a_0 c I_R \left(1 - \frac{S_V}{N_R}\right)\Bigg)^T \end{aligned} \tag{9}$$

it is clear that $\hat{G}(X,Z) > 0$, therefore from ([38]), we get the result.

10.4. Appendix D. Basic Reproduction Number Calculation

Define $\mathcal{F}$ as the column-vector of rates of the appearance of new infections in each compartment; $\mathcal{V} = \mathcal{V}^+ + \mathcal{V}^-$, where $\mathcal{V}^+$ is the column-vector of rates of transfer of individuals into the particular compartment; and $\mathcal{V}^-$ is the column-vector of rates of transfer of individuals out of the particular compartment. The matrices F and V can be calculated from the partial derivatives of $\mathcal{F}$ and $\mathcal{V}$ with respect to the infected classes computed at the DFE.

From the model (1),

$$\mathcal{F} = \begin{pmatrix} a_0 b I_V \frac{S_H}{N_H} \\ 0 \\ 0 \\ 0 \\ 0 \\ a_0 b I_V \frac{S_R}{N_R} \\ \mu_1 a_0 c S_V \frac{I_A}{N_H} + a_0 c S_V \left(\frac{I_H + P_H}{N_H}\right) + \mu_2 a_0 c S_V \frac{I_R}{N_R} \end{pmatrix}$$

and

$$\mathcal{V} = \begin{pmatrix} (\gamma_e + \mu_h)E_H \\ (\gamma_h + \mu_h)I_A - f_1\gamma_e E_H \\ (\alpha_1 + \delta + \mu_h)I_H - (1-f_1)\gamma_e E_H - \rho_1\gamma_h I_A \\ (\delta_p + \mu_H)T_H - (1-\sigma)\alpha_1 I_H \\ (\alpha_2 + \beta + \mu_h)P_H - \rho_2\gamma_h I_A - \delta_p T_H \\ \mu_r I_R \\ \mu_v I_V \end{pmatrix}.$$

Then the matrices $\mathbf{F}$ and $\mathbf{V}$ from the partial derivatives of $\mathcal{F}$ and $\mathcal{V}$ with respect to the infected classes computed at the DFE are given by

$$\mathbf{F} = \begin{pmatrix} 0 & 0 & 0 & 0 & 0 & 0 & a_0 b \\ 0 & 0 & 0 & 0 & 0 & 0 & 0 \\ 0 & 0 & 0 & 0 & 0 & 0 & 0 \\ 0 & 0 & 0 & 0 & 0 & 0 & 0 \\ 0 & 0 & 0 & 0 & 0 & 0 & a_0 b \\ 0 & \mu_1 a_0 cm & a_0 cm & 0 & a_0 cm & \mu_2 a_0 cn & 0 \end{pmatrix}$$

and

$$\mathbf{v} = \begin{pmatrix} \gamma_e + \mu_h & 0 & 0 & 0 & 0 & 0 & 0 \\ -f_1\gamma_e & \gamma_h + \mu_h & 0 & 0 & 0 & 0 & 0 \\ -(1-f_1)\gamma_e & -\rho_1\gamma_h & \alpha_1 + \delta + \mu_h & 0 & 0 & 0 & 0 \\ 0 & 0 & -(1-\sigma)\alpha_1 & \delta_p + \mu_H & 0 & 0 & 0 \\ 0 & -\rho_2\gamma_h & 0 & -\delta_p & \alpha_2 + \beta + \mu_h & 0 & 0 \\ 0 & 0 & 0 & 0 & 0 & \mu_r & 0 \\ 0 & 0 & 0 & 0 & 0 & 0 & \mu_v \end{pmatrix}$$

10.5. Appendix E. Details about the Model calibration

The initial human demographic parameters $S_H(0)$, $E_H(0)$, $I_H(0)$, $P_H(0)$, $T_H(0)$, $R_H(0)$ as well as initial infected reservoir population $I_R(0)$, initial infected sandfly population $I_V(0)$ are also estimated. It is assumed that $I_A(0) = N_H(0) - S_H(0) - E_H(0) - I_H(0) - T_H(0) - P_H(0) - R_H(0)$ and $T_H(0) = C(0) - I_H(0) - P_H(0)$.

The carrying capacity (N_V) of the sandfly population is assumed to be a multiple of the total human population at the beginning i.e. $N_V(0) = k_2 \times N_H(0)$, where k_2 is the total number of sandfly per human.

Similarly, initially $N_R(0) = k_1 \times N_H(0)$, where k_1 is the total number of reservoir per human. The author estimates k_1 and k_2

from the given data of Visceral Leishmaniasis. Initial susceptible sandfly population $S_V(0) = N_V(0) - I_V(0)$ and initial susceptible reservoir population $S_R(0) = N_R(0) - I_R(0)$.

The author adds an extra compartment to the model (1), to calculate the cumulative number of new notified VL infections I_C, by

$$\frac{dI_C}{dt} = (1 - f_1)\gamma_e E_H + \rho_1 \gamma_h I_A + (1 - \sigma)\alpha_1 I_H + \delta_p T_H + \rho_2 \gamma_h I_A$$

which is the rate of new case. The numerical solutions of the above equation with the model (1) give the predicted monthly cumulative VL incidence. Here, $I_C(0)$= number of new notified cases at the first time point of the data (C(0)).

The sum of the squared error between the model and data should be minimized, which is given by

$$RSS = \Sigma_{i=1}^{n}(z_i - g_i(t_i, \widehat{\theta}))^2,$$

where z_i is the cumulative VL data, and $g_i(t_i, \widehat{\theta}) = I_C(t_i, \widehat{\theta}) + \epsilon$, $\epsilon \sim N(0, I\sigma^2)$ where $t_i = 0, 31, ..., 365$ days, and ϵ be the error of fit, which follows an independent Gaussian distribution having unknown variance σ^2. MCMC tool box in MATLAB written by Marko Laine ([39]) was used to estimate the unknown $\widehat{\theta}$ for the model (1). Geweke's Z-scores ([40]) were used to ensure the chain convergence.

REFERENCES

[1] A. Stauch, H. Duerr, J. Dujardin, M. Vanaerschot, S. Sundar, and M. Eichner. Treatment of visceral leishmaniasis: model-based analyses on the spread of antimony-resistant L. donovani in bihar, india. *PLOS Neglected Tropical Diseases*, 6(12):e1973, 2012.

[2] WHO. Leishmaniasis fact sheet, 2014. URL http://www.who.int/mediacentre/factsheets/fs375/en.

[3] R. W. Ashford. The leishmaniases as emerging and reemerging zoonoses. *International Journal for Parasitology*, 30(12):1269–1281, 2000.

[4] B. Ostyn, K. Gidwani, B. Khanal, A. Picado, F. Chappuis, S. Singh, S. Rijal, S. Sundar, and M. Boelaert. Incidence of symptomatic and asymptomatic Leishmania donovani infections in high-endemic foci in india and nepal: a prospective study. *PLOS Neglected Tropical Diseases*, 5(10): e1284, 2011.

[5] S. Sundar, R. Singh, R. Maurya, B. Kumar, A. Chhabra, V. Singh, and M. Rai. Serological diagnosis of indian visceral leishmaniasis: direct agglutination test versus rk39 strip test. *Transactions of the Royal Society of Tropical Medicine and Hygiene*, 100(6):533–537, 2006.

[6] A. Stauch, R. Sarkar, A. Picado, B. Ostyn, S. Sundar, S. Rijal, M. Boelaert, J. Dujardin, and H. Duerr. Visceral leishmaniasis in the indian subcontinent: modelling epidemiology and control. *PLOS Neglected Tropical Diseases*, 5(11):e1405, 2011.

[7] L. Stockdale and R. Newton. A review of preventative methods against human leishmaniasis infection. *PLOS Neglected Tropical Diseases*, 7(6):e2278, 2013.

[8] S. Joshi, K. Rawat, N. K. Yadav, V. Kumar, M. I. Siddiqi, and A. Dube. Visceral leishmaniasis: Advancements in vaccine development via classical and molecular approaches. *Frontiers in Immunology*, 5:380, 2014.

[9] C. Dye and D. Wolpert. Earthquakes, influenza and cycles of indian kala-azar. *Transactions of the Royal Society of Tropical Medicine and Hygiene*, 82(6):843–850, 1988.

[10] C. Dye. The logic of visceral leishmaniasis control. *The American Journal of Tropical Medicine and Hygiene*, 55(2): 125–130, 1996.

[11] L. Chaves and M. Hernandez. Mathematical modelling of american cutaneous leishmaniasis: incidental hosts and threshold conditions for infection persistence. *Acta Tropica*, 92(3):245–252, 2004.

[12] P. Das and A. Sarkar. Effect of delay on the model of american cutaneous leishmaniasis. *Journal of Biological Systems*, 15 (2):139–147, 2007.

[13] I. Elmojtaba, J. Mugisha, and M. Hashim. Mathematical analysis of the dynamics of visceral leishmaniasis in the sudan. *Applied Mathematics and Computation*, 217(6):2567–2578, 2010.

[14] A. Mubayi, C. Castillo-Chavez, G. Chowell, C. Kribs-Zaleta, N. Siddiqui, N. Kumar, and P. Das. Transmission dynamics and underreporting of kala-azar in the indian state of bihar. *Journal of Theoretical Biology*, 262(1):177–185, 2010.

[15] E. Agyingi, D. Ross, and K. Bathena. A model of the transmission dynamics of leishmaniasis. *Journal of Biological Systems*, 19(2):237–250, 2011.

[16] A. Stauch, H. Duerr, A. Picado, B. Ostyn, S. Sundar, S. Rijal, M. Boelaert, J. Dujardin, and M. Eichner. Model-based investigations of different vector-related intervention strategies to eliminate visceral leishmaniasis on the indian subcontinent. *PLOS Neglected Tropical Diseases*, 8(14):e2810, 2014.

[17] K. S. Rock, E. A. le Rutte, S. J. de Vlas, E. R. Adams, G. F. Medley, and T. D. Hollingsworth. Uniting mathematics and biology for control of visceral leishmaniasis. *Trends in Parasitology*, 31(6):251–259, 2015.

[18] D. Lewis. The biology of phlebotomidae in relation to leishmaniasis. *Annual Review of Entomology*, 19(1):363–384, 1974.

[19] M. Burattini, F. Coutinho, L. Lopez, and E. Massad. Modelling the dynamics of leishmaniasis considering human, animal host and vector populations. *Journal of Biological Systems*, 6(4):337–356, 1998.

[20] B. Lee, K. Bacon, M. Shah, S. Kitchen, D. Connor, and R. Slayton. The economic value of a visceral leishmaniasis vaccine in bihar state, india. *The American Journal of Tropical Medicine and Hygiene*, 86(3):417–425, 2012.

[21] S. Biswas, A. Subramanian, I. Elmojtaba, J. Chattopadhyay, and R. Sarkar. Optimal combinations of control strategies and cost-effective analysis for visceral leishmaniasis disease transmission. *PLOS ONE*, 12(2):e0172465, 2017.

[22] V. Gandhi, N. S. Al-Salti, and I. M. Elmojtaba. Mathematical analysis of a time delay visceral leishmaniasis model. *Journal of Applied Mathematics and Computing*, 63(1):217–237, 2020.

[23] O. Diekmann, J. A. P. Heesterbeek, and J. A. J. Metz. On the definition and computation of the basic reproduction ratio r_0 in models for infectious diseases in heterogeneous populations. *Journal of Mathematical Biology*, 28:365–382, 1990.

[24] P. Van den Driessche and J. Watmough. Reproduction numbers and the sub-threshold endemic equilibria for compartmental models of disease transmission.

Mathematical Biosciences, 180:29–48, 2002.

[25] J. Carr. *Applications of Centre Manifold Theory*. Springer-Verlag, New York, 1981.

[26] C. Castillo-Chavez and B. Song. Dynamical models of tuberculosis and their applications. *Mathematical Biosciences and Engineering*, 1(2):361–404, 2004.

[27] A. Abubakar, J. A. Ruiz-Postigo, J. Pita, M. Lado, R. Ben-Ismail, D. Argaw, and J. Alvar. Visceral leishmaniasis outbreak in south sudan 2009–2012: epidemiological assessment and impact of a multisectoral response. *PLOS Neglected Tropical Diseases*, 8(3):e2720, 2014.

[28] S. Marino, I. B. Hogue, C. J. Ray, and D. Kirschner. A methodology for performing global uncertainty and sensitivity analysis in systems biology. *Journal of Theoretical Biology*, 254:178–196, 2008.

[29] G. Pedruzzi, P. N. Das, K.V.S. Rao, and S. Chatterjee. Understanding pge2, lxa4 and ltb4 balance during mycobacterium tuberculosis infection through mathematical model. *Journal of theoretical biology*, 389:159–170, 2016.

[30] P. N. Das, G. Pedruzzi, N. Bairagi, and S. Chatterjee. Coupling calcium dynamics and mitochondrial bioenergetic: an in silico study to simulate cardiomyocyte dysfunction. *Molecular BioSystems*, 12(3):806–817, 2016.

[31] The World Bank. South sudan country data, 2012. URL http://data.worldbank.org/country/south-sudan.

[32] S. Sundar, D. Lockwood, G. Agrawal, M. Rai, M. Makharia, and H. Murray. Treatment of indian visceral leishmaniasis with single or daily infusions of low dose liposomal amphotericin b. *BMJ*, 323(7310):419–422, 2001.

[33] S. Gasim, A. Elhassan, A. Kharazmi, E. Khalil, A. Ismail, and T. Theander. The development of post-kala-azar dermal leishmaniasis (pkdl) is associated with acquisition of leishmania reactivity by peripheral blood mononuclear cells (pbmc). *Clinical and Experimental Immunology*, 119 (3):523–529, 2000.

[34] L. A. Chapman, L. Dyson, O. Courtenay, R. Chowdhury, C. Bern, G. F. Medley, and T. D. Hollingsworth. Quantification of the natural history of visceral leishmaniasis and consequences for control. *Parasites & Vectors*, 8(1):1–13, 2015.

[35] S. Srivastava, P. Shankar, J. Mishra, and S. Singh. Possibilities and challenges for developing a successful vaccine for leishmaniasis. *Parasites & Vectors*, 9(1):277, 2016.

[36] K. Jain and N. Jain. Vaccines for visceral leishmaniasis: A review. *Journal of Immunological Methods*, 422:1–12, 2013.

[37] F. B. Agusto. Mathematical model of ebola transmission dynamics with relapse and reinfection. *Mathematical Biosciences*, 283:48–59, 2017.

[38] C. Castillo-Chavez, Z. Feng, and W. Huang. *On the computation of R_0 and its role on global stability*, volume 125. Institute for Mathematics and its Applications, 2001.

[39] M. Laine. *Adaptive MCMC methods with applications in environmental and geophysical models*. PhD thesis, Finnish Meteorological Institute, 2008.

[40] J. Geweke. Evaluating the accuracy of sampling-based approaches to the calculation of posterior moments. Technical Report 148, Federal Reserve Bank of Minneapolis, 1991.